A statistical analysis of well production rates from UK oil and gas fields – Implications for carbon capture and storage

Simon A. Mathias[1], Jon G. Gluyas[1], Eric J. Mackay[2], Ward H. Goldthorpe[3]

1. Department of Earth Sciences, Durham University, Durham, UK

2. Institute of Petroleum Engineering, Heriot Watt University, Edinburgh, UK

3. Carbon Capture and Storage Programme, The Crown Estate, London, UK

Abstract

The number of wells required to dispose of global CO_2 emissions by injection into geological formations is of interest as a key indicator of feasible deployment rate, scale and cost. Estimates have largely been driven by forecasts of sustainable injection rate from mathematical modelling of the CO_2 injection process. Recorded fluid production rates from oil and gas fields can be considered an observable analogue in this respect. The article presents statistics concerning Cumulative average Bulk fluid Production (CBP) rates per well for 104 oil and gas fields from the UK offshore region. The term bulk fluid production is used here to describe the composite volume of oil, gas and water produced at reservoir conditions. Overall, the following key findings are asserted: (1) CBP statistics for UK offshore oil and gas fields are similar to those observed for CO_2 injection projects worldwide. (2) 50% probability of non-exceedance (PNE) for CBP for oil and gas fields without water flood is around 0.35 Mt/yr/well of CO_2 equivalent. (3) There is negligible correlation between reservoir transmissivity and CBP. (4) Study of net and gross CBP for water flood fields suggest a 50% PNE that brine co-production during CO_2 injection could lead to a 20% reduction in the number of wells required.

Introduction

There has been on-going discussion in the literature concerning the number of injection wells that will be needed to store global CO_2 emissions in geological formations (Ehlig-Economides and Economides, 2010; Cavanagh et al., 2010; 2011; Hosa et al., 2011; Gammer et al., 2011). Confidence concerning estimates of number of wells required can be increased by consideration of previous experience. However, commercial-scale CO_2 injection data remains scarce (Michael et al., 2010; Michael et al., 2011; Hosa et al., 2011). Consequently, current estimates heavily rely on numerical simulation (e.g., Pickup et al., 2011; Jin et al., 2012, Zhou et al., 2012). A particular issue with numerical simulation concerns the excessive grid-resolution required to ensure numerically converged results (Pickup et al., 2012). This in turn leads to prohibitive computational requirements in the context of sensitivity analysis for uncertainty propagation (Mathias et al., 2013a; Hedley et al., 2013) although this problem can be partially alleviated by the use of simplified analytical solutions (e.g. Mathias et al., 2011b; Mathias et al., 2013b).

This article seeks to gain further insight concerning the estimation of CO_2 injection rates by undertaking a statistical analysis of production data from 119 UK offshore oil and gas fields (DECC, 2013) (see Figure 1). The conclusions from this work provide new information for forecasting likely injection rates, and therefore numbers of wells, for future CO_2 storage projects located on the UK continental shelf.

The article commences with an explanation concerning the need and methodology for converting data for standard conditions (60^oF and 14.7 psi) to an equivalent combined volumetric flow rate of oil, gas and water at reservoir conditions. A discussion is then provided to explain the choice of using the cumulative average production rate after 10 years. Production data statistics for UK offshore oil and gas fields are compared with those for CO_2 injection projects world-wide. Water

flood data are used to gain further insights concerning the usefulness of brine co-production during CO_2 injection. An investigation is then performed to look at how production statistics vary for different reservoir types. Finally, the article summarises and concludes.

Formatting of DECC production data

Time series data for all UK offshore oil and gas fields can be obtained from DECC (2013) (UK Department of Energy and Climate Change) including both monthly production and injection data for oil, gas and water. An example of such a data set is shown for the Balmoral oil field in Figure 2a. The DECC (2013) data is reported at standard conditions (SC), i.e., 60^oF and 14.7 psi (Ahmed, 2001, p. 33). Also note to obtain an average production rate per production well it is necessary to divide the DECC (2013) data by the number of production wells in the field. For example, the Balmoral field has 14 production wells (DECC, 2007).

Note that the number of production wells in a given field often increases with field life. However, the history of well development for each field studied was not available for this investigation.

At reservoir conditions (RC) the solubility of gas in oil is much higher. Once the oil is brought to SC, the gas solubility is significantly reduced and gas comes out of solution. Most of the gas produced in UK oil fields has been derived by this process. In reservoir engineering it is typical to quantify gas solubility in terms of a gas-oil-ratio at SC, R_s, which is measured in standard cubic ft of gas per standard barrel of oil (SCF/BBL). Figure 3a shows a plot of R_s as a function of pressure for the Balmoral field, assuming a correlation function presented by Glaso (1980) (see Eq. 2.73 of Ahmed, 2001). Note that beyond 1460 psi, R_s remains constant. This critical pressure for a given oil and gas is referred to as the bubble point, defined as the pressure at which a bubble of gas appears on depressurising.

Also of interest is the gas expansion factor, E_g (-), defined as the volume of gas at SC divided by the volume of gas at RC. Figure 3a also shows E_g (-) for Balmoral according to the Peng and Robinson (1977) equation of state (EOS) assuming critical pressures and temperatures as calculated using the correlations of Standing (1977) (see Eqs. 2.18 and 2.19 of Ahmed, 2001). Note that E_g increases with increasing reservoir pressure due to the increase in gas density associated with compression.

A unit volume of oil at RC results in a smaller produced volume at SC due to the loss of gas from solution when the pressure is lowered. Also, at RC, once gas is dissolved an increase in reservoir pressure leads to a slight reduction in oil volume due to compression of the oil phase. The oil formation volume factor, B_o (-), is defined as the volume of oil at RC divided by the resulting volume of oil at SC. Figure 3a shows a plot of B_o as a function of pressure for Balmoral, assuming another correlation function presented by Glaso (1980) (see Eq. 2.87 of Ahmed, 2001), to account for gas exsolution, in conjunction with the correlation of Spivey et al. (2007), to account for oil compression. Above the bubble point, as pressure decreases, B_o increases because the volume of oil is increasing in the reservoir due to decompression. However, once bubble point is reached, B_o decreases with decreasing pressure because gas within the oil is coming out of solution.

Note that in principle, B_o should go to unity as pressure approaches 14.7 psi. This is not the case for Glaso's correlation because the analysis is based only on experimental data observed at bubble point pressure. Nevertheless, Glaso's correlation is considered to be one of the more accurate correlations available (Ahmed, 2001, Chapter 2) and is pertinent to our study given that is based on oils exclusively from the North Sea. Furthermore, in the analysis that follows, the formation volume factors are applied at initial reservoir pressures, which are typically above or near bubble point.

The blue line in Figure 2b shows monthly oil production at RC. This was obtained by multiplying monthly oil production at SC by the formation volume factor, B_o, based on the initial reservoir pressure. Also of interest is the cumulative average rate (in green). This gives information concerning how the lifetime average rate changes with time. It is clear that there is a gradual decline in the cumulative average oil production rate, which is due to the depletion of the oil within the reservoir.

However, to draw insights concerning CO_2 injection, it is of greater interest to consider an estimate of bulk (i.e., oil, gas and water) monthly fluid production at RC, V_b (BBL), found from

$$V_b = B_o V_o + (V_g - R_s V_o)/E_g + B_w V_w \quad (1)$$

where V_o (BBL), V_g (SCF), V_w (BBL) are the monthly productions of oil, gas and water, respectively, at SC and B_w (-) is the formation water volume factor (similar to B_o but for formation water). The formation water volume factor can be obtained by consideration of the density correlations presented by Batzle and Wang (1992).

Cumulative average Bulk fluid Production, $\overline{V_b}$, (CBP) for Balmoral is shown as a red line in Figure 2b. As can be seen, $\overline{V_b}$ is virtually independent of the oil production rate and dependent more on the water injection that occurs during the first 10 years (compare Figure 2a).

Another quantity of interest is the net bulk fluid production, $V_{b,net}$ (BBL), which is found from

$$V_{b,net} = V_b - V_{g,inj}/E_g - B_w V_{w,inj} \quad (2)$$

where $V_{g,inj}$ (SCF), $V_{w,inj}$ (BBL) are the monthly injections of gas and water, respectively, at SC.

Cumulative average net bulk fluid production, $\overline{V}_{b,net}$, for Balmoral is shown as a turquoise line in Figure 2b. Again it can be said that, $\overline{V}_{b,net}$ is virtually independent of the oil production rate. However, net fluid production is negative at the beginning of operations due to large quantities of water injection. But after 20 years, net fluid production starts to converge although still exhibiting a moderate decline. This latter decline may be due to constraints associated with fluid production in the reservoir associated with bulk transmissivity and compressibility of the reservoir as a whole. Alternatively, it could also be case that the decline is due to increasing water cut in the producers, thus increasing the gravity head in the well and thereby reducing the flow rates or even leading to lift die out in some wells.

It is reasonable to compare the net CBP with an equivalent CO_2 injection rate. Assuming a CO_2 density of 629 kg/m^3 (quite representative of CO_2 density at reservoir conditions), it can be said that 1 Mt will take up a volume of 10 million barrels (MMBBL).

However, the following caveats should be understood:

(1) Although a correction has been made in terms of fluid density, the above analysis ignores effects associated with differences (between CO_2 and the originally produced fluids) in fluid compressibility and viscosity.

(2) For oil/gas production, production rates are often reduced with respect to the maximum possible production rates for reservoir management reasons (such as avoiding early water or gas breakthrough). It is not clear for how many of the 104 datapoints this is the case.

(3) For oil/gas production, the production could be well constrained (notably lift problems after water breakthrough) rather than reservoir constrained. It is not clear for how many of the 104 fields this is the case. Also, for production, a relatively small tubing size may have been selected to avoid lift problems later on in the field life. For CO_2 injection, tubing size is still a consideration, but optimal tubing size could be larger.

The Balmoral field is convenient in this context. However, the Ninian field represents a more problematic example. Production history and estimates of cumulative average production rates for Ninian are shown in Figure 4. The first issue is that, for the first ten years, the CBP is less than the cumulative average oil production (compare red and green lines in Figure 4b). This is because no gas production (or water production for that matter) was reported for that period (see green line in Figure 4a) although gas must have been produced with the oil (consider the $(V_g - R_s V_o) / E_g$ term in Eq. (1)). The next problem is that towards the end of the field life, as much fluid is being injected as produced so as to continue oil production. Consequently the net CBP is virtually zero towards the end.

Parameters required for the Glaso (1980), Peng and Robinson (1977), Standing (1977), Spivey et al. (2007) and Batzle and Wang (1992) correlations include reservoir temperature, T (^{o}F), initial reservoir pressure, P (psi), specific gravity of the gas (relative to air at SC), γ_g (-), oil gravity, API (^{o}API), the gas oil ratio at bubble point, R_{sb} (SCF/BBL), and water salinity, SAL (ppm NaCl eq.).

For many of the fields listed in DECC (2013), most of the parameters described above can be found from Abbots (1991) and/or Gluyas and Hichens (2003) (both of these documents are referred to hereafter as AGH). However, special considerations include γ_g and R_{sb}.

For fields with a specified gas expansion factor, E_g, a value for γ_g is calculated by iterative solution of the Peng and Robinson (1977) EOS, otherwise the AGH γ_g value is assumed.

A value of R_{sb} is obtained by assuming reservoir pressure is initially above bubble point and calculating R_{sb} based on the mean of the first four months of SC oil and gas production data. The Glaso (1980) correlation is then used to estimate the bubble point pressure. If the estimated bubble point pressure is less than the initial reservoir pressure, the aforementioned value of R_{sb} is accepted. Alternatively, the reported bubble point pressure from the AGH dataset is used with the Glaso (1980) correlation to calculate an alternative estimate of R_{sb}. If none of the above is possible, the R_s value reported in AGH is assumed to be R_{sb}.

Where pressure data is absent, a hydrostatic pressure gradient is assumed. Where reservoir temperature is absent, a geothermal gradient of 0.0179 ^{o}F/ft with a surface temperature of 52.8 ^{o}F is assumed (obtained by linear regression of the AGH temperature and depth to crest data). Where γ_g, API and SAL are absent, mean values for the AGH dataset are assumed. Mean values of γ_g, API and SAL for all the fields reported in AGH are 0.794, 36.9^{o}API and 126,000 ppm NaCl eq., respectively.

Note that this mean value of salinity is not realistic for some reservoirs. The Permian and some of the Upper Jurassic are near salt saturation whereas some other reservoirs in the Upper Jurassic are much less at around 70,000 ppm and the Brent is less saline than sea water (Warren and Smalley, 1994). However, the SAL parameter is only required for calculation of B_w, the sensitivity of which, in comparison to expansions associated with the oil and gas, is virtually negligible. It was necessary to apply the mean value of salinity to 20 of 104 reservoirs.

Statistical analysis of DECC production data

Cumulative distributions for the CBP data from DECC (2013) are shown in Figure 5. The data have been separated out into oil fields without water flood, gas fields and oil fields with water flood. Note that for the fields with water flood, both gross and net production data are presented (Figs 5c and d, respectively). Also note that these data are production rate per well. This has been obtained by dividing the field-scale data, as discussed in the previous section, by the number of production wells in the field. The number of production well data has been obtained from DECC (2007) and the AGH dataset. Probability of non-exceedance (PNE) has been calculated using the Weibull plotting position (Makkonen, 2006).

The data in Fig. 5 have been further separated to show how CBP statistics vary with production time. The statistics for the oil fields without water flood are relatively stationary with time (Figure 5a). The remainder of the fields exhibit relative stationary statistics for the first 10 to 15 years and then trend towards a reduced production rate, with the exception of the 25 years production for the gas field data (Fig 5b.). However, the latter should not be considered in too much detail as there are only two recorded gas fields that produced for that duration.

Another way to visualise the data is to consider Figure 6a, which shows plots of CBP against production time for the four categories displayed in Figures 5a-d for PNE of 30%, 50% and 70%. Here it can be seen that the categories in order of decreasing 50% PNE CBP are gas fields, oil fields without water flood and oil fields with water flood. Plotted alongside in Figure 6b are the number of fields active for a given production time, from which it can be seen that there is a moderate correlation between the decline in production rate after 15 years and a decline in the number of fields active after 15 years.

Comparison with CO_2 injection data

Figure 7a compares the cumulative distributions of CBP, after 10 years of production, for oil fields without water flood, gas fields and oil fields with water flood (net production) with injection rate data from CO_2 storage projects from around the world. The latter data was obtained from Table 4 of Hosa et al. (2011) for 15 projects including Sleipner, Snohvit, Weyburn and In Salah. Hosa et al. (2011) report mass injection rates in tonnes per day. These are converted to MMBBL/yr by assuming a CO_2 density of 629 kg/m^3 such that 1 Mt = 10 MMBL, as discussed above. The 50% PNE for net CBP for the oil fields, gas fields and water flood fields are 3.51, 3.38 and 0.416 MMBL/yr/well, respectively. The good (high injection rate per well) CO_2 projects are similar to the good gas fields. The more limited CO_2 projects are similar to the oil fields with water flood.

Hosa et al. (2011) also reports corresponding reservoir transmissivities (i.e., permeability × formation thickness). Similar data are available for the oil and gas reservoirs from AGH. Figure 7b compares plots of CBP against transmissivity for oil fields without water flood, gas fields and oil fields with water flood alongside the CO_2 injection data from Hosa et al. (2011). Interestingly, gas fields are clustered in the lower right of the plot. This may be largely due to the lower viscosity of gas as compared with oil. However, overall it can be said that there is very little correlation between production/injection rate with transmissivity. Nevertheless, it is interesting to note that distribution of CO_2 injection data shares a similar space to the DECC production data. Overall, Figures 7a and b provide a good basis for using the oil and gas production data to provide additional insights concerning future CO_2 injection rates.

It should be understood that many of the CO_2 injection rates in the Hosa et al. (2011) study are constrained by factors other than injectivity. Sleipner is constrained to 1 MT/year due to plant design. Weyburn is an EOR (Enhanced Oil Recovery) operation where the amount of CO_2 injected is driven by optimisation of oil recovery and CO_2 price. Furthermore, many of the low-rates are

attributed to small-scale test projects where testing of monitoring technologies was a main focus (e.g. Ketzin). Nevetherless, the Hosa et al. (2011) study represents a useful reflection concerning injection rates that have actually been achieved to date.

Insights from water flooding

The number of injection wells required for a given CO_2 storage site can be reduced by implementing pressure relief via nearby brine production wells (Cavanagh et al., 2010; Neal et al., 2011). However, the effectiveness of pressure relief by brine production is strongly dependent on reservoir connectivity (Neal et al., 2011). Furthermore, Neal et al. (2011) show, through numerical modelling, that brine production only becomes economically beneficial in this context when brine production leads to a greater than 10% reduction in the number of required wells. The water flood data discussed above can be used to explore this issue further.

Taking the net CBP as a lower bound estimate of the gross CBP that would have occurred in the absence of water flood, an upper bound estimate of productivity improvement factor, as a consequence of water flood, can be obtained by considering the ratio of gross fluid production to net fluid production. This factor can then be used to indicate a possible increase in CO_2 injectivity one would get in the same reservoir when implementing brine production.

A comparison of gross production with net production for water flood fields after 10 years of production is presented in Figure 8a. This represents data from a total of 57 oil fields. The 50% PNE for net and gross CBP are 0.416 and 1.40 MMBBL/yr/well, respectively, which, in effect, quantifies the improvement in productivity obtained by water flooding. Interestingly, the data also suggests an 8.6% probability of not exceeding zero net CBP. This is because some of the fields have negative net CBP (consider again Figure 4b).

Figure 8b shows the cumulative distribution for the ratio of gross to net CBP. Note that for ease of interpretation, fields with negative net CBP have been excluded from Figure 8b, which is conservative in this context. The results in Figure 8b indicate a 50% probability of not exceeding (or exceeding) a gross to net CBP ratio of 2.5. Assuming one injection well for every production well, this can be shown to correspond to a predicted reduction in number of wells due to brine production of 20%. Furthermore, a 10% reduction in number of wells corresponds to a gross to net CBP ratio of 2.22, which, according to Figure 8b, corresponds to a PNE of 42.6%. Combining Figure 8b with the analysis of Neal et al. (2011) in turn leads to the idea of a 57.4% probability that brine co-production during CO_2 injection, in the UK offshore region, is likely to be economically beneficial.

Most of the water flood fields would have yielded higher CBP unaided than their net CBP with water injection. For example at Ninian (recall Figure 4b), net CBP was negative. Obviously, Ninian would have yielded a positive CBP unaided. Therefore it should be realised that the ratio of gross to net CBP is likely to be an overestimate of injectivity improvement (due to water flooding) for many of the fields included. This overestimation has been partially mitigated by the exclusion of fields with negative net CBP. Nevertheless, it would be unwise to interpret the extreme values in Figure 8b in this context.

Possible performance indicators

Figure 7b shows that there is very little correlation between production rate and transmissivity. Other important aspects include the size of the reservoir compartment and connectivity to outer aquifer systems (Zhou et al., 2008; Mathias et al., 2011a; 2013a; Chang et al., 2013). Within the AGH dataset, the various oil and gas reservoirs are designated a structure type. Terms applied for a

given reservoir include: structural; stratigraphic/unconformity; four-way dip antiform/anticline; four-way closure over salt diaper, tilted fault block; three-way dip & fault; faulted pericline; faulted rollover; updip pinch-out; combined stratigraphic/structural; combined tilted and inverted fault block and combined anticline and stratigraphic. We have consolidated these further to just four categories: structural; 4-way closure; with a fault seal; and stratigraphic/structural. Figure 9 shows how reservoir productivity partitions out for the four categories. The statistics are almost identical for each category except for stratigraphic/structural, which come out with better production rates.

Interestingly, the AGH dataset comments on reservoir mechanisms. Mechanism designations include: pressure depletion drive; gas cap expansion drive; aquifer/natural water drive; gravity drive; water flood/water injection; combined aquifer and gas expansion drive; combined aquifer drive and gas injection; combined water injection, gas injection and depressurization; gas recycle; combined full voidage replacement and water injection; combined depletion and water flood; combined aquifer drive and water injection. We have consolidated these further to just three categories: no aquifer; aquifer drive; and water flood. Figure 10 shows how reservoir productivity partitions out for three mechanism designations. Here it can be seen that where there is no water injection, there is little difference between statistics associated with reservoirs with and without aquifer drive.

Fields selected for water flood exhibited significantly lower net CBP rates compared with fields not employing water injection. In part this is a function of the way in which fields under water flood are managed. Typically, the early phase of production is through depletion drive and consequential pressure drop. The pressure drop is commonly halted just above bubble point through water injection. The field is then managed at just above bubble point. The reason for doing this is to minimise the energy required for injection while avoiding the problems associated with relative permeability loss if gas starts to break-out within the reservoir. Consequently, when we examine old

fields with very long injection and production phases, the overall net volume change in the reservoir can be very small (Figure 5d), particularly in instances where late field life has been accompanied by overvoidage (e.g. Figure 4).

Another interesting indicator is reservoir age. Figure 11 shows how reservoir productivity partitions out for different geological ages. Of note is that the Triassic and, albeit to a lesser extent, the Permian reservoirs have statistically better productivity that the remainder. Both these sets of fields; Permian gas fields of the Southern North Sea and Triassic oil and gas fields of the Central and Southern North Sea respectively have been developed with depletion drive alone. As such the Permian and Triassic data are likely to be a better indicator of long term injectivity potential for CO_2.

The slight difference between the Jurassic (poorer) and Cretaceous/Tertiary performance may be a reflection of the larger unbroken sandstone bodies of the Cretaceous/Tertiary relative to the older reservoirs.

Summary and conclusions

The objective of this article was to present a statistical investigation concerning production rates in UK offshore oil and gas reservoirs, with a view to gaining further insight concerning forecasting of likely injection rates for similarly located CO_2 storage projects in the future. Production data was sourced from DECC (2013), which reports field-scale monthly production and injection of oil, gas and water. These data are reported at standard conditions. So as to compare to possible CO_2 injection rates, it was necessary to convert these data to reservoir conditions and integrate into a net Cumulative averaged Bulk fluid Production (CBP). This was achieved by virtue of the fluid properties data presented in Abbotts (1991) and Gluyas and Hichens (2003) (referred to collectively

as AGH) in conjunction with correlations presented by Batzle and Wang (1992), Glaso (1980), Peng and Robinson (1977), Spivey et al. (2007) and Standing (1977). Assuming a CO_2 density of 629 kg/m^3, 1 Mt of CO_2 is equivalent to a CBP of 10 MMBL. Note that the term bulk fluid production is used here to describe the composite volume of oil, gas and water produced at reservoir conditions.

It was found that CBP statistics became temporally less stable after between 10 and 15 years of production (Figure 5). Furthermore, it was found that the number of active oil and gas fields started to decline significantly after 15 years of production (Figure 6). It was therefore decided to consider CBP after 10 years of production for the remainder of the study. CBP statistics were then compared to existing CO_2 injection data (after Hosa et al., 2011) (Figure 7). It was found that net CBP from water flood fields was significantly less than from gas fields and oil fields without water flood. The largest and smallest CO_2 injection rates were found to be similar to net CBP for the largest gas field and smallest water flooded fields, respectively. The 50% probability of non-exceedance (PNE) for net CBP for the oil fields, gas fields and water flood fields were 3.51, 3.38 and 0.416 MMBL/year/well, respectively, which equates to around 0.35, 0.34 and 0.04 Mt/year/well of CO_2 equivalent, respectively.

The 50% PNE for gross CBP in the water flood fields was 1.40 MMBL/year/well. The improvement on productivity due to water flooding was investigated further by studying the statistics of gross to net CBP ratio for the water flood fields. Improved productivity leads to reductions in the number of wells required. In the same way, brine co-production during CO_2 injection is thought to lead to reduced numbers of wells for CO_2 storage operations. The 50% PNE gross to net CBP ratio for the water flood fields was 2.5 (Figure 8b). Assuming one injection well for every production well, this corresponds to an equivalent reduction in number of wells of 20%. Numerical work by Neal et al. (2011) suggests that brine co-production becomes economically

beneficial for CO_2 storage operations, providing this leads to a reduction in number of wells of more than 10%.

CBP was found to have very little correlation with reservoir transmissivity. Through a study of alternative variables including reservoir structure, reservoir mechanism and reservoir age, it was found that reservoir mechanism and reservoir age had the strongest control on CBP. In terms of reservoir mechanism, those reservoirs selected for water flood exhibited significantly reduced net and gross CBP as compared to other reservoirs. In terms of reservoir age, the Triassic and Permian reservoirs had the highest CBP. However, this may be largely due to the fact that less reservoirs in the Triassic and Permian were selected for water flood.

Overall, the following key findings can be asserted: (1) CBP statistics for UK offshore oil and gas fields are similar to those observed for CO_2 injection projects worldwide. (2) The 50% PNE for CBP for oil and gas fields without water flood is around 0.35 Mt/yr/well of CO_2 equivalent. (3) There is negligible correlation between reservoir transmissivity and CBP. (4) Study of net and gross CBP for water flood fields suggest a 50% PNE that brine co-production during CO_2 injection could lead to 20% reduction in the number of wells required.

Acknowledgments

This work was funded by The Crown Estate. We are grateful to Liam Herringshaw for help collating some of the AGH data. We are also grateful for useful improvements to the text provided by two anonymous reviewers from IJGGC.

References

415 Abbotts, I. L. (1991). United Kingdom oil and gas fields: 25-years commemorative volume (No.
416 14). Geological Society Pub House.
417 Ahmed, T. (2001). Reservoir engineering handbook. Second Edition. Gulf Professional Publishing.
418 London.
419 Batzle, M., & Wang, Z. (1992). Seismic properties of pore fluids. Geophysics, 57(11), 1396-1408.
420 Cavanagh, A. J., Haszeldine, R. S., & Blunt, M. J. (2010). Open or closed? A discussion of the
421 mistaken assumptions in the Economides pressure analysis of carbon sequestration. Journal
422 of Petroleum Science and Engineering, 74(1), 107-110.
423 Chang, K. W., Hesse, M. A., & Nicot, J. P. (2013). Reduction of lateral pressure propagation due to
424 dissipation into ambient mudrocks during geological carbon dioxide storage. Water
425 Resources Research. 49, 2573-2588.
426 Ehlig-Economides, C., & Economides, M. J. (2010). Sequestering carbon dioxide in a closed
427 underground volume. Journal of Petroleum Science and Engineering, 70(1), 123-130.
428 DECC (2007) BERR Well Production
429 https://www.og.decc.gov.uk/information/wells/pprs/Well_production_offshore_oil_fields/offshore_
430 oil_fields_by_well/offshore_oil_fields_by_well.htm
431 DECC (2013) UK Monthly Oil Production. https://www.og.decc.gov.uk/pprs/full_production.htm
432 Gammer, D., Green, A., Holloway, S., & Smith, G. (2011). The Energy Technologies Institute's UK
433 CO2 storage appraisal project (UKSAP).
434 Glaso, O. (1980). Generalized pressure-volume-temperature correlations. Journal of Petroleum
435 Technology, 32(5), 785-795.
436 Gluyas, J. G., & Hichens, H. M. (Eds.). (2003). United Kingdom oil and gas fields: commemorative
437 millennium volume (No. 20). Geological Society.
438 Hedley, B. J., Davies, R. J., Mathias, S. A., Hanstock, D., & Gluyas, J. G. (2013). Uncertainty in
439 static CO2 storage capacity estimates: Case study from the North Sea, UK. Greenhouse
440 Gases: Science and Technology.

441 Hosa, A., Esentia, M., Stewart, J., & Haszeldine, S. (2011). Injection of CO2into saline formations:
442 Benchmarking worldwide projects. Chemical Engineering Research and Design, 89(9),
443 1855-1864.
444 Jin, M., Pickup, G., Mackay, E., Todd, A., Sohrabi, M., Monaghan, A., & Naylor, M. (2012). Static
445 and Dynamic Estimates of CO2-Storage Capacity in Two Saline Formations in the UK. SPE
446 Journal, 17(4), 1108-1118.
447 Makkonen, L. (2006). Plotting positions in extreme value analysis. Journal of applied meteorology
448 and climatology, 45(2), 334-340.
449 Mathias, S. A., de Miguel, G. J. G. M., Thatcher, K. E., & Zimmerman, R. W. (2011a). Pressure
450 buildup during CO2 injection into a closed brine aquifer. Transport in porous media, 89(3),
451 383-397.
452 Mathias, S. A., Gluyas, J. G., González Martínez de Miguel, G. J., & Hosseini, S. A. (2011b). Role
453 of partial miscibility on pressure buildup due to constant rate injection of CO2 into closed
454 and open brine aquifers. Water Resources Research, 47(12).
455 Mathias, S. A., Gluyas, J. G., González Martínez de Miguel, G. J., Bryant, S. L., & Wilson, D.
456 (2013a). On relative permeability data uncertainty and CO2 injectivity estimation for brine
457 aquifers. International Journal of Greenhouse Gas Control, 12, 200-212.
458 Mathias, S. A., & Roberts, A. W. (2013b). A Lambert W function solution for estimating
459 sustainable injection rates for storage of CO2in brine aquifers. International Journal of
460 Greenhouse Gas Control.
461 Michael, K., Golab, A., Shulakova, V., Ennis-King, J., Allinson, G., Sharma, S., & Aiken, T.
462 (2010). Geological storage of CO2in saline aquifers—A review of the experience from
463 existing storage operations. International Journal of Greenhouse Gas Control, 4(4), 659-667.
464 Michael, K., Neal, P. R., Allinson, G., Ennis-King, J., Hou, W., Paterson, L., ... & Aiken, T. (2011).
465 Injection strategies for large-scale CO2storage sites. Energy Procedia, 4, 4267-4274.

Neal, P. R., Cinar, Y., & Allinson, W. G. (2011). The economics of pressure-relief with CO2injection. Energy Procedia, 4, 4215-4220.

Peng, D. Y., & Robinson, D. B. (1977). A rigorous method for predicting the critical properties of multicomponent systems from an equation of state. AIChE Journal, 23(2), 137-144.

Pickup, G. E., Jin, M., & Mackay, E. J. (2012, September). Simulation of Near-Well Pressure Build-up in Models of CO2 Injection. In ECMOR XIII-13th European Conference on the Mathematics of Oil Recovery.

Pickup, G., Jin, M., Olden, P., Mackay, E., & Sohrabi, M. (2011, May). A Sensitivity Study on CO2 Storage in Saline Aquifers. In SPE EUROPEC/EAGE Annual Conference and Exhibition.

Spivey, J., Valko, P., & McCain, W. (2007). Applications of the Coefficient of Isothermal Compressibility to Various Reservoir Situations With New Correlations for Each Situation. SPE Reservoir Evaluation & Engineering, 10(1), 43-49.

Standing, M. B., (1977) Volumetric and Phase Behavior of Oil Field Hydrocarbon Systems, pp. 125–126. Dallas: Society of Petroleum Engineers.

Warren, E. A., & Smalley, P. C. (Eds.). (1994). North Sea formation waters atlas (No. 15). Geological Society Publishing House.

Zhou, Q., Birkholzer, J. T., Tsang, C. F., & Rutqvist, J. (2008). A method for quick assessment of CO2 storage capacity in closed and semi-closed saline formations. International Journal of Greenhouse Gas Control, 2(4), 626-639.

Zhao, R., Cheng, J., & Zhang, K. (2012). CO2 Plume Evolution and Pressure Buildup of Large-scale CO2 Injection into Saline Aquifers in Sanzhao Depression, Songliao Basin, China. Transport in Porous Media, 95(2), 407-424.

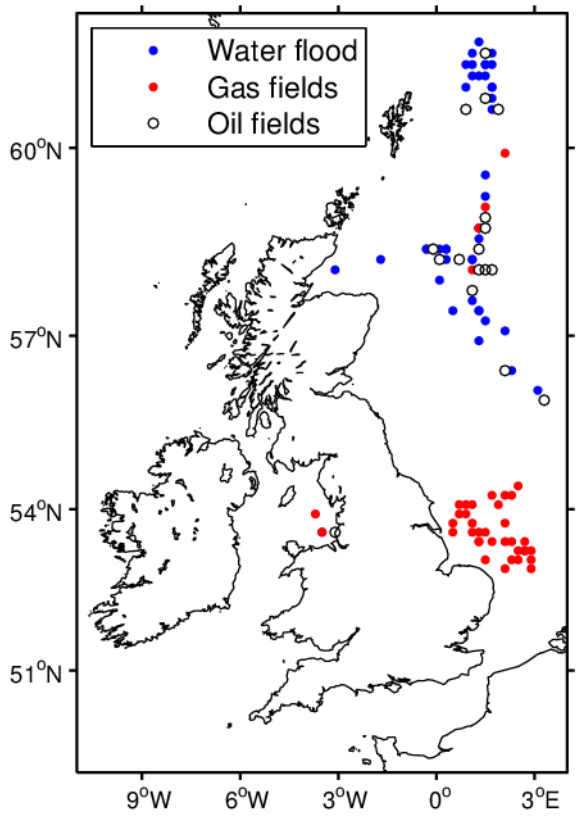

Figure 1: Map of UK showing locations of the oil and gas fields studied. In the legend, “water flood” refers to oil fields where water injection has been used and “oil fields” refer to oil fields where water injection has not been used.

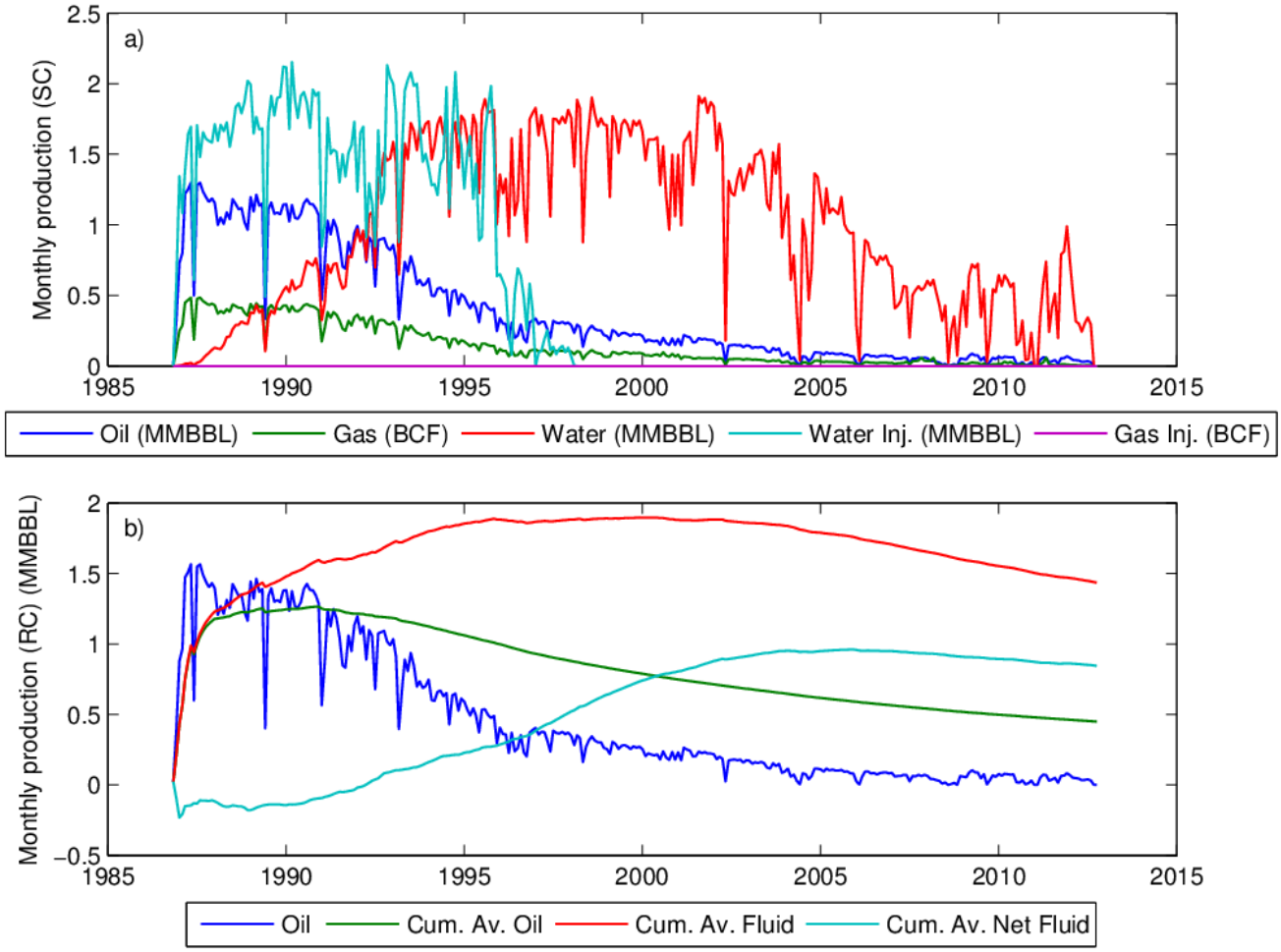

499

500 Figure 2: Time series plot of monthly production for the Balmoral field. a) Assuming standard
501 conditions (SC). Note that data here are production data except for “Water Inj.” and “Gas Inj.”,
502 which are injection data. b) Assuming reservoir conditions (RC). Note that “Cum. Av.” is an
503 abbreviation for cumulative average and “Net Fluid” involves subtracting the injected water and
504 gas.

505

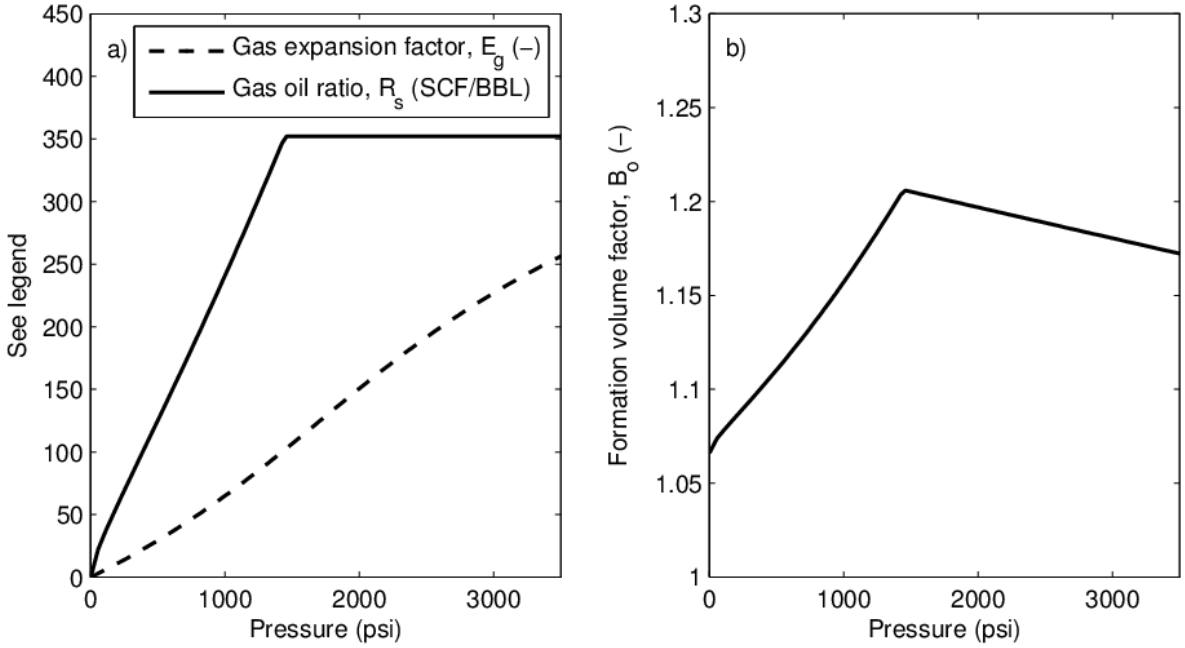

506

507 Figure 3: Plots of gas expansion factor, gas oil ratio and formation volume factor against pressure,

508 as assumed for the Balmoral field. Assumed associated parameters include $T = 207\ ^{o}\text{F}$, $\gamma_g = 0.79$,

509 API = 39.9, $R_{sb} = 352$ SCF/BBL.

510

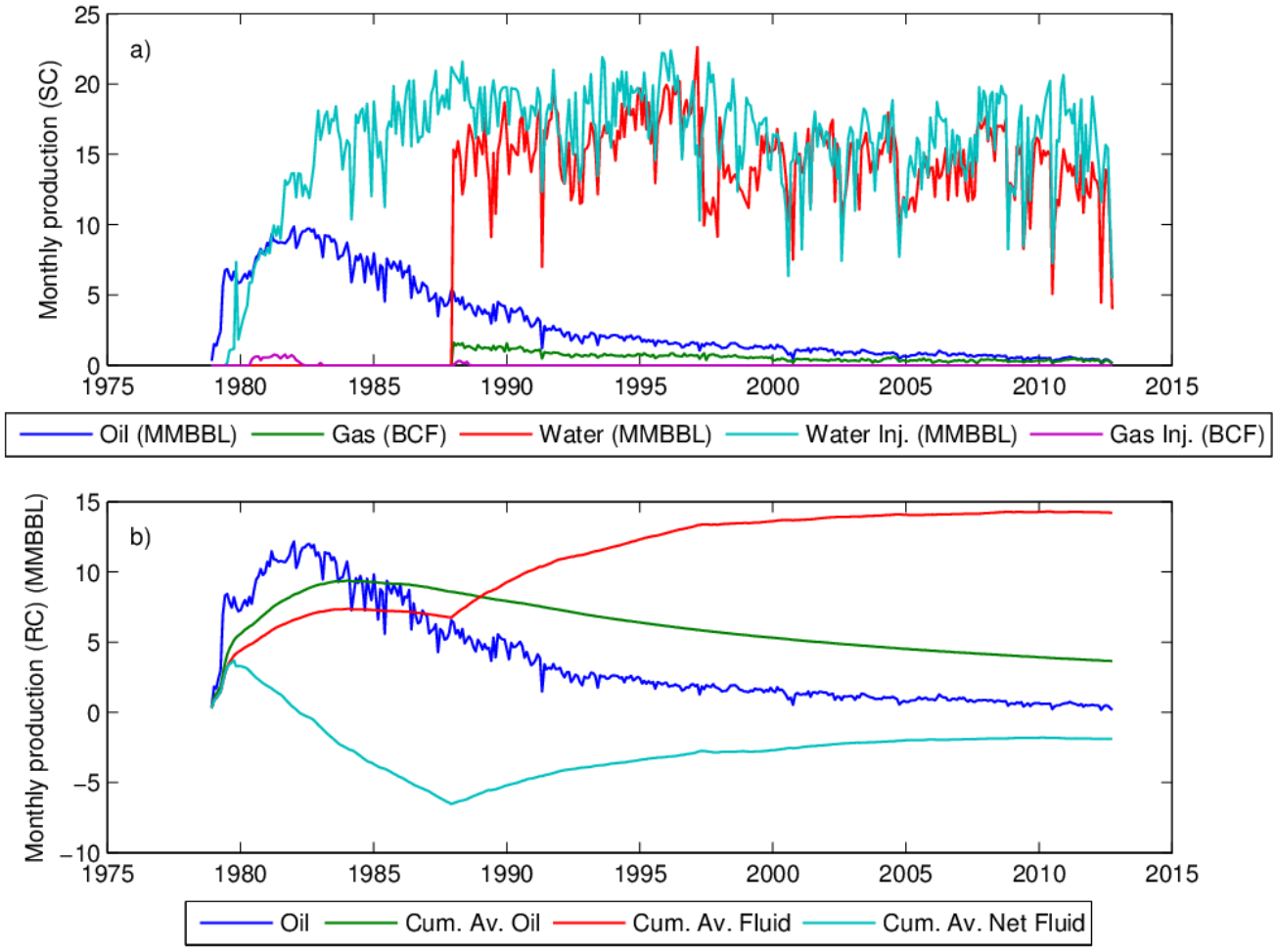

511

512 Figure 4: Same as Figure 2 but for the Ninian field.

513

514

515

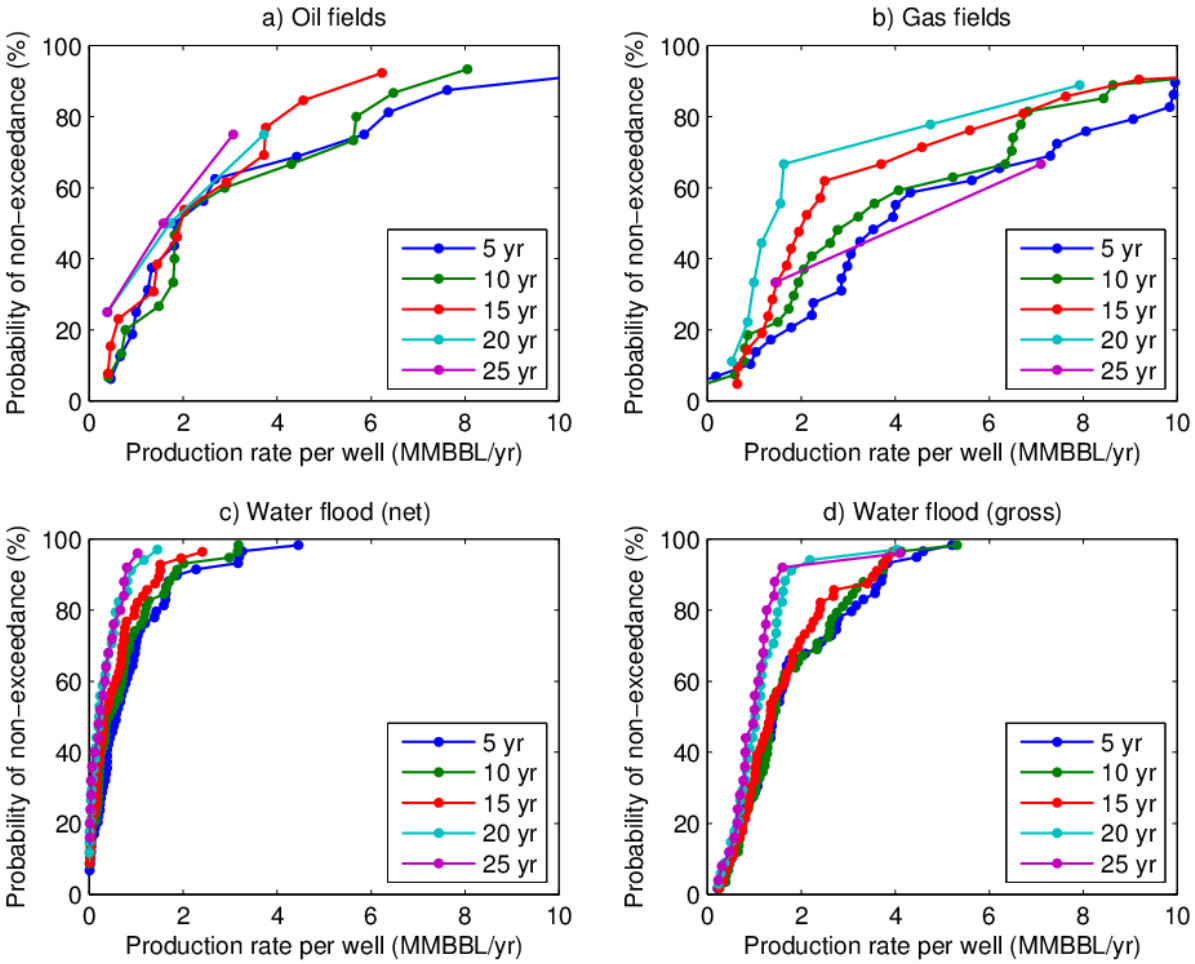

516

517 Figure 5: Cumulative distribution plots for net CBP rate (at RC) per well for varying production
518 times (as indicated in legend). a) Oil fields. b) Gas fields. c) Net production for oil fields with water
519 flood. d) Gross production for oil fields with water flood.

520

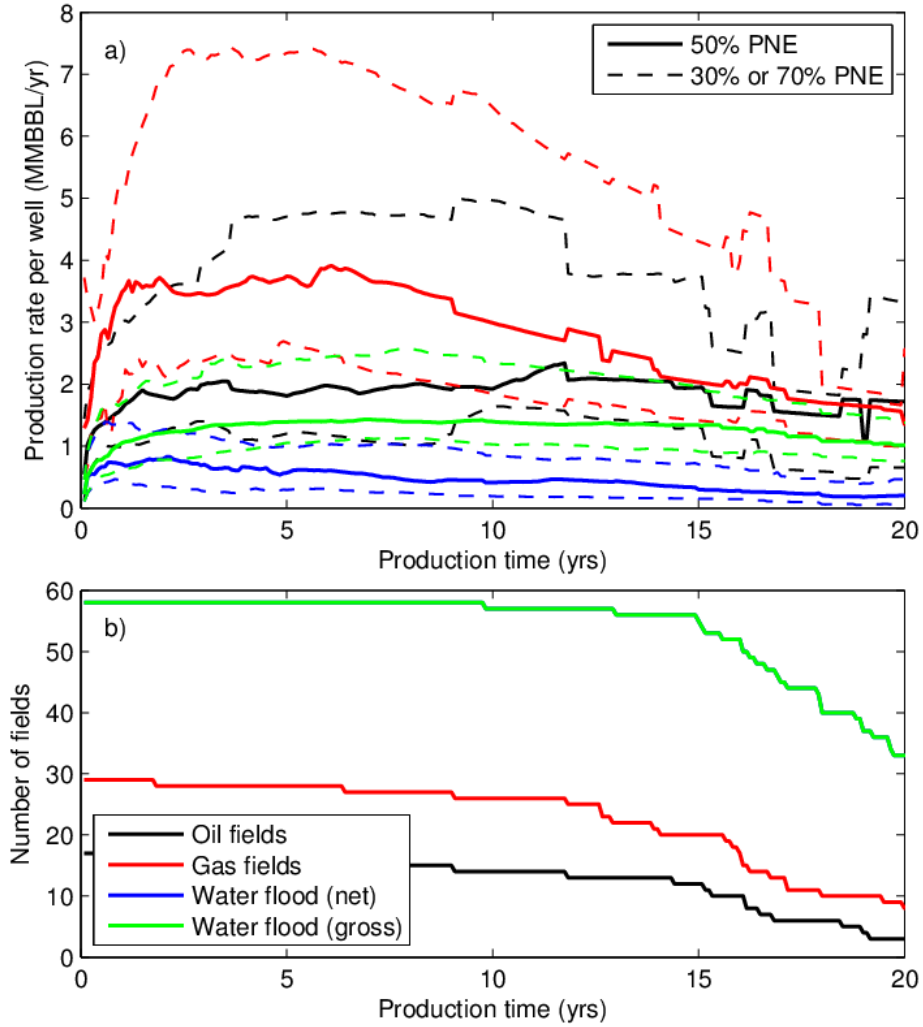

Figure 6: a) Plot of 30, 50 and 70 probability of non-exceedance (PNE) for net CBP rate (at RC) per well against production time for oil fields, gas fields and oil fields with water flood (both net and gross production rates), as indicated by the legend in Figure 5b. b) Plot of number of fields active for a given production time for the three categories: oil fields, gas fields and oil fields with water flood.

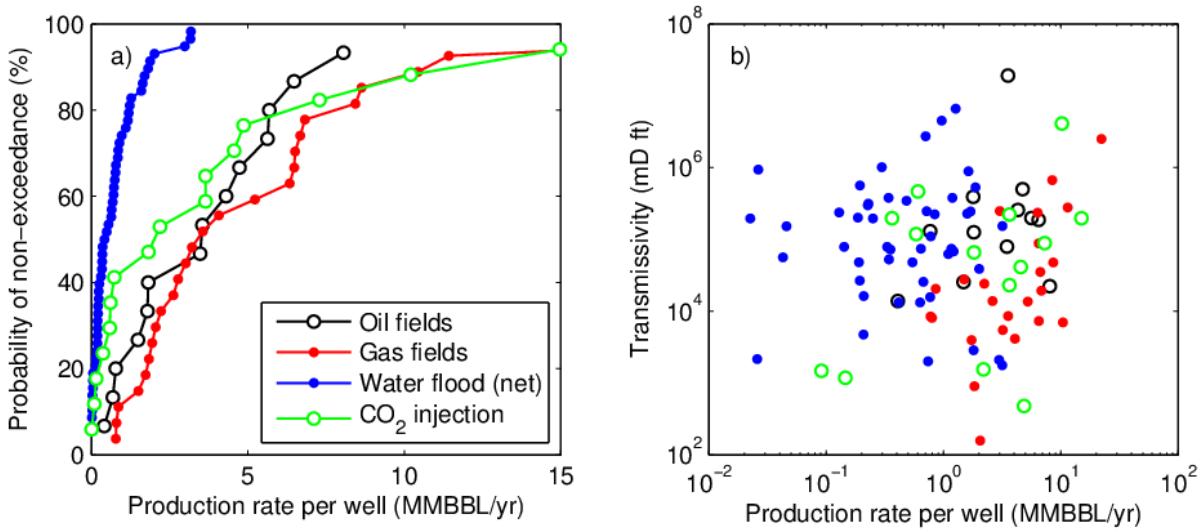

Figure 7: a) Cumulative distribution plots for net CBP rate (at RC) per well after 10 years of production for the oil fields without water flood, gas fields and oil fields with water flood and the CO_2 injection data reported by Hosa et al (2011) (assuming a CO_2 density of 629 kg/m^3 such that 1 Mt/yr = 10 MMBBL/yr). b) The same production data but plotted against the transmissivities of the reservoirs. Transimssivity is calculated using net thickness with the exception of those data provided by Hosa et al. (2011), which used gross thickness.

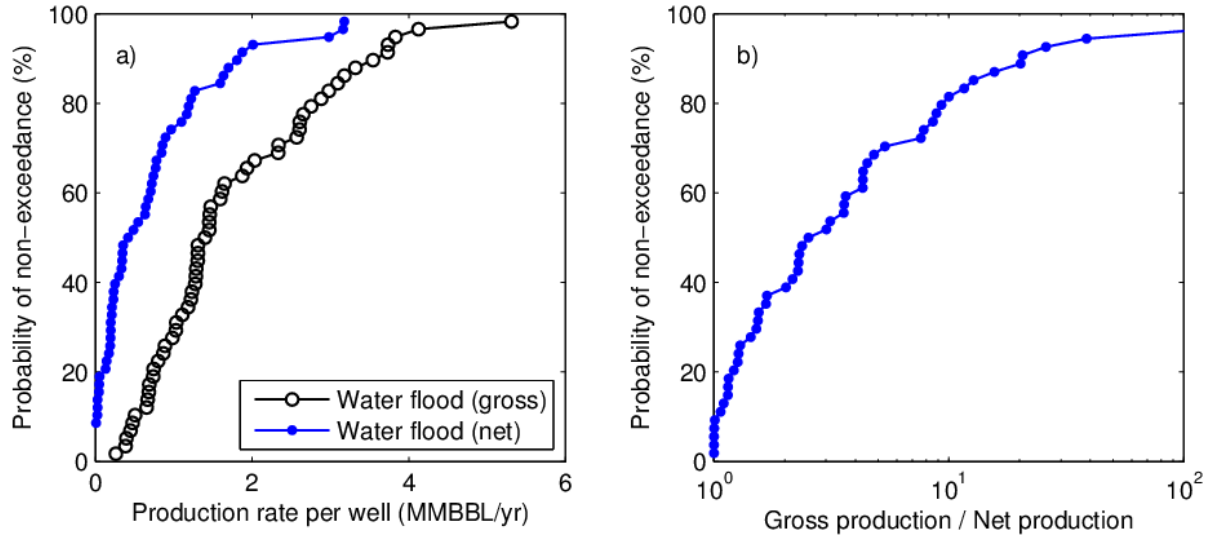

Figure 8: a) Cumulative distribution plots for CBP rate (at RC) per well after 10 years of production for the oil fields with water flood, both gross and net production rates. b) Cumulative distribution plot for the ratio of gross to net CBP for oil fields with water flood.

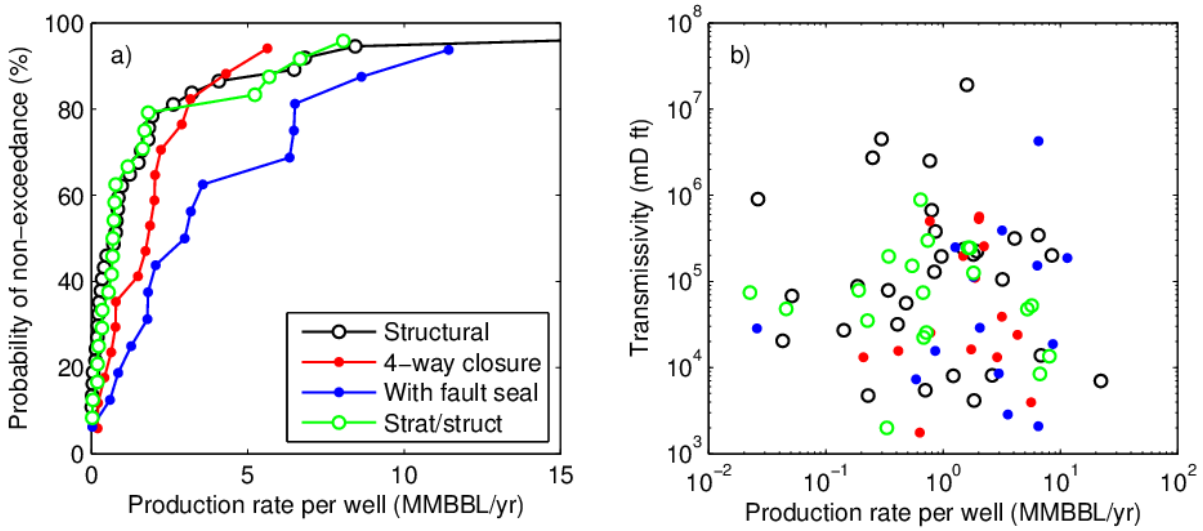

542

543 Figure 9: Same as Figure 7 but separated out in terms of reservoir structure type.

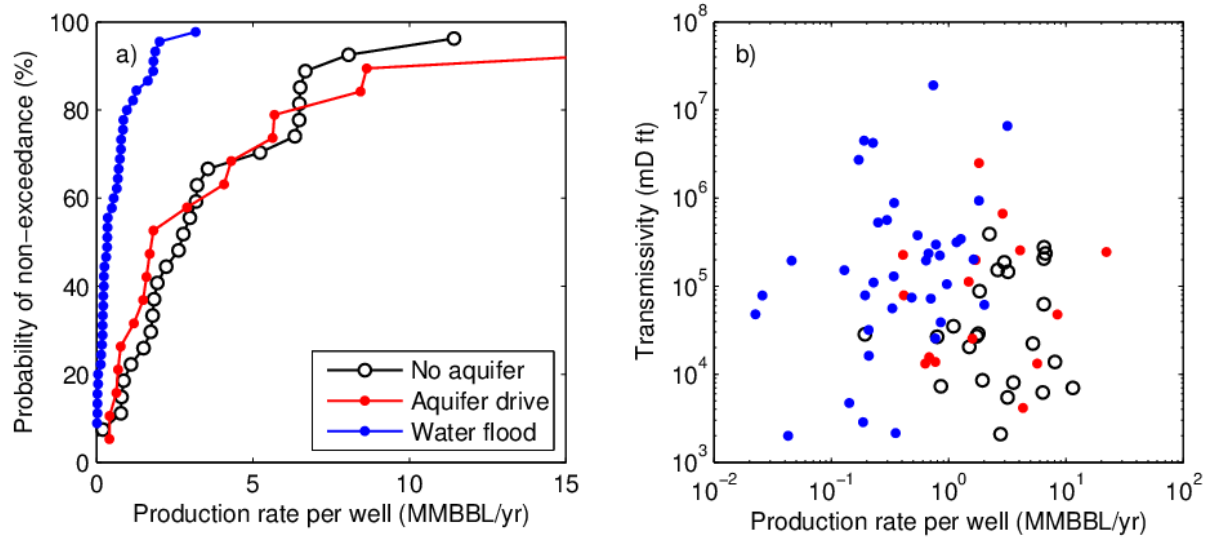

544

545 Figure 10: Same as Figure 7 but separated out in terms of designated reservoir mechanism.

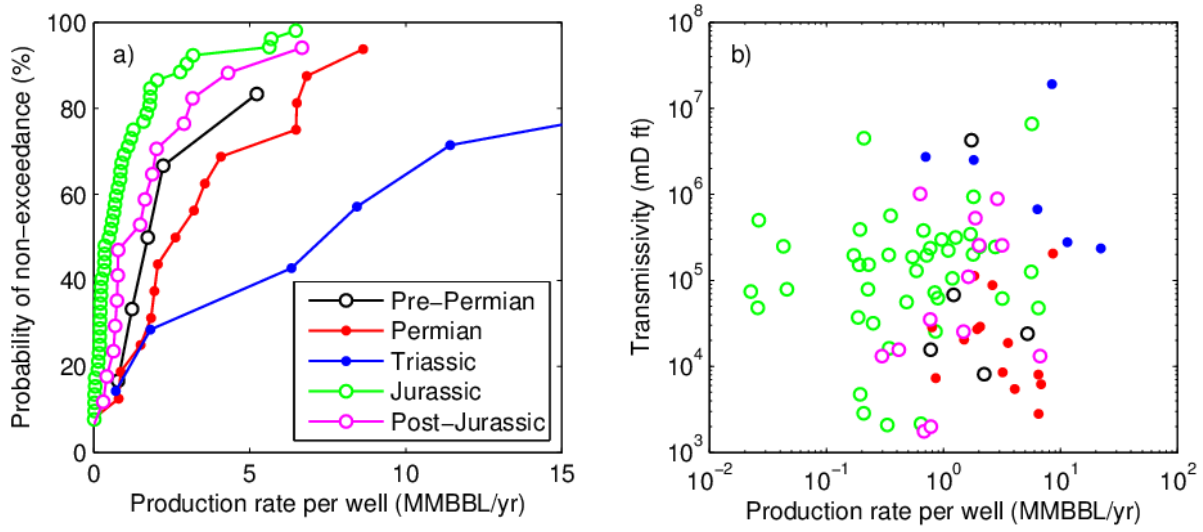

546

547 Figure 11: Same as Figure 7 but separated out in terms of reservoir age.